

Supporting Information

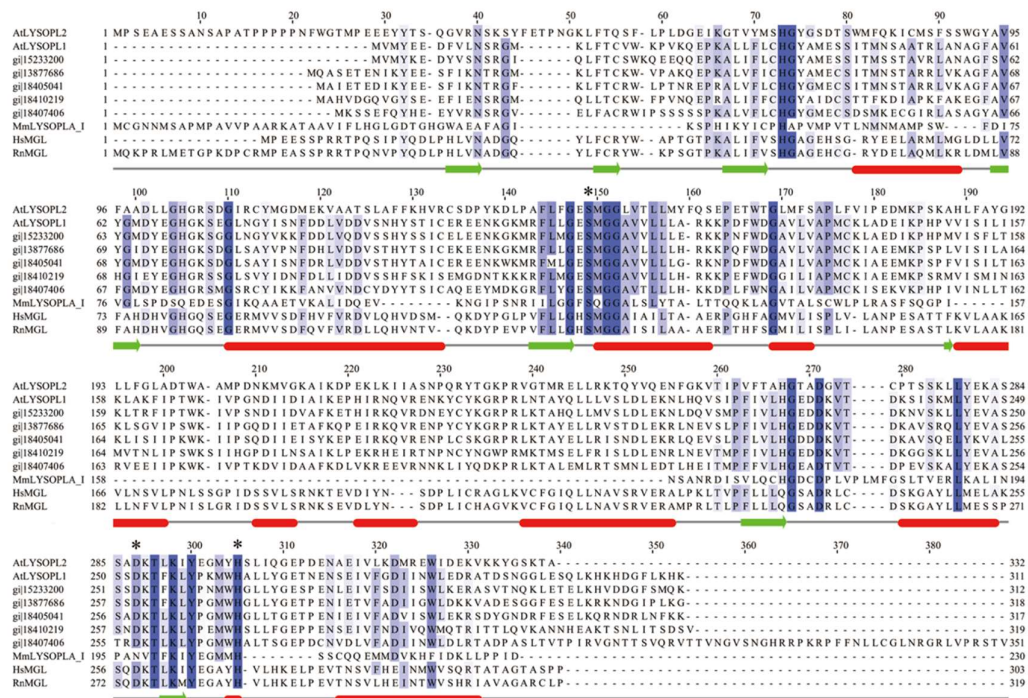


Figure S-1. Structure-based alignment using software Jalview version 1.6. Structure-based alignment of AtLYSOPL2, AtLYSOPL1, AtLYSOPL1-like proteins (gi15233200, gi13877686, gi18405041, gi18410219, gi18407406), *M. musculus* LysoPLA I, *H. sapiens* MGL, and *R. norvegicus* MGL. Identical amino acid residues are marked in dark blue, homologous residues in light blue, and gaps as dashes; α-helices (red lines) and β-strands (green lines) are indicated below the sequences. The conserved catalytic residues (Ser-147, Asp-268 and His-298) are marked with asterisks.

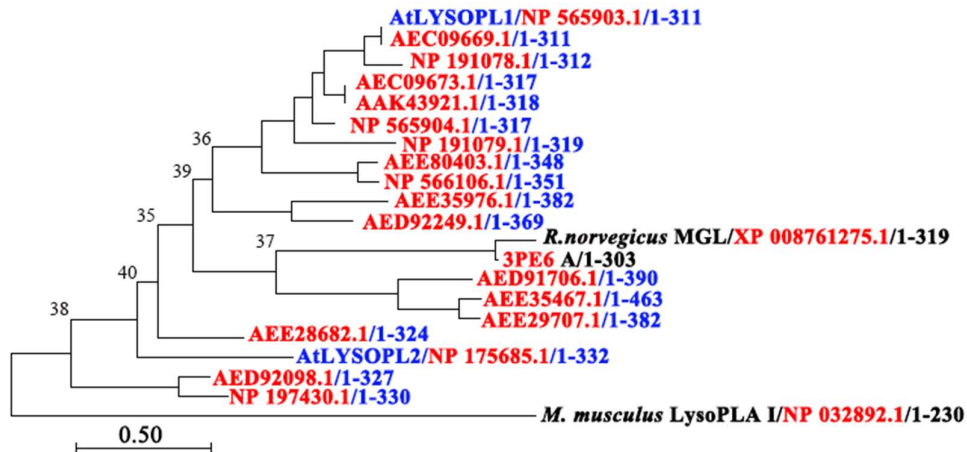


Figure S-2. Molecular phylogenetic analysis of LysoPL homologues. AtLYSOPL2, AtLYSOPL1, AtLYSOPL1-like proteins, *M. musculus* LysoPLA I, *H. sapiens* MGL, *R. norvegicus* MGL and *Arabidopsis* monoacylglycerol lipases (MAGL) were analyzed by the Maximum Likelihood method. The protein accession numbers are as follow: AtLYSOPL2 (NP_175685.1), AtLYSOPL1 (NP_565903.1), AtLYSOPL1-like proteins (NP_191078.1, AAK43921.1, NP_565904.1, NP_191079.1 and NP_566106.1), *M. musculus* LysoPLA I (NP_032892.1), *H. sapiens* MGL (3PE6_A), *R. norvegicus* MGL (XP_008761275.1) and *Arabidopsis* MAGL (AEE28682.1, AEE29707.1, AEE35467.1, AEE35976.1, AEC09669.1, NP_565904.1, AEC09673.1, NP_566106.1, NP_191078.1, NP_191079.1, AEE80403.1, AED91706.1, AED92098, AED92249.1 and NP_197430.1). Bootstrap values (> 35%) are recorded at the nodes. *Arabidopsis* proteins are denoted in blue, and protein accession numbers in red.

Reference

Jones, D. T., Taylor, W.R., and Thornton, J.M. (1992) The rapid generation of mutation data matrices from protein sequences. *Comput. Appl. Biosci.* **8**, 275-82

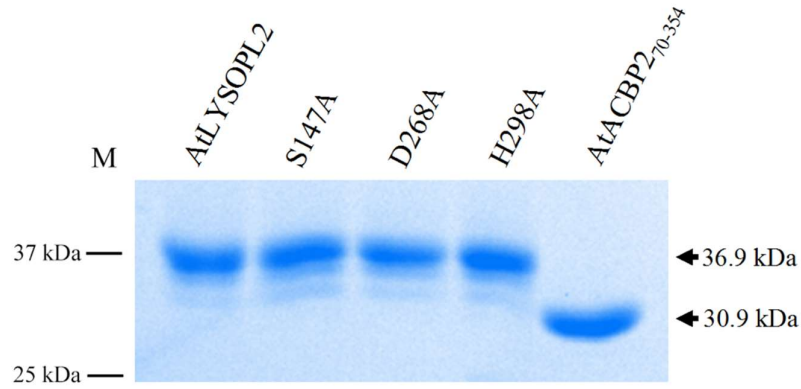


Figure S-3. SDS-polyacrylamide gel electrophoresis of the purified AtLYSOPL2 (wild type), AtLYSOPL2 mutant proteins (S147A, D268A, H298A) and AtACBP2₇₀₋₃₅₄. Eluted fractions of AtLYSOPL2 (wild type), AtLYSOPL2 (S147A), AtLYSOPL2 (D268A), AtLYSOPL2 (H298A) and AtACBP2₇₀₋₃₅₄ were collected. Arrows indicate homogeneity of the purified proteins. The predicted molecular weights of AtLYSOPL2 and AtACBP2₇₀₋₃₅₄ protein are 36.9 kDa and 30.9 kDa, respectively. M, protein marker.

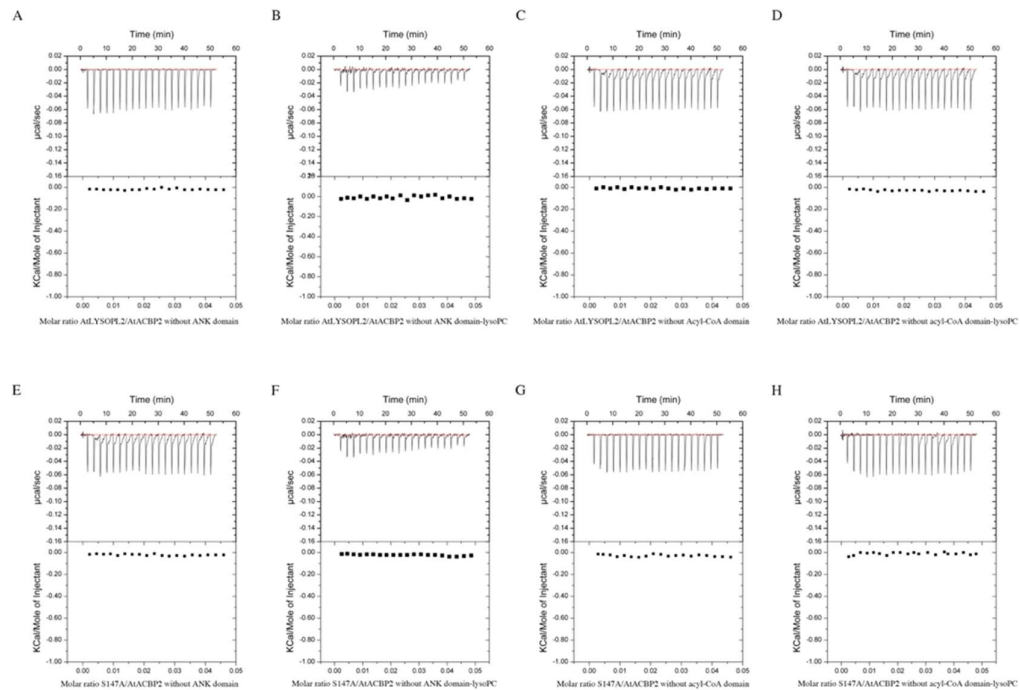


Figure S-4. ITC analysis of interactions of AtLYSOPL2 wild-type or its mutant (S147A) with AtACBP2₇₀₋₂₁₄ or AtACBP2₂₁₅₋₃₅₄ with/without lysoPC. (A-B) Wild-type AtLYSOPL2 with AtACBP2₇₀₋₂₁₄ alone (A) or complexed with lysoPC (B). AtACBP2₇₀₋₂₁₄ consists of the ACB domain lacking ankyrin repeats. (C-D) Wild-type AtLYSOPL2 with AtACBP2₂₁₅₋₃₅₄ alone (C) or complexed with lysoPC (D). (E-F) AtLYSOPL2 mutant (S147A) with AtACBP2₇₀₋₂₁₄ (E) or complexed with lysoPC (F). (G-H) AtLYSOPL2 mutant (S147A) with AtACBP2₂₁₅₋₃₅₄ alone (G) or complexed with lysoPC (H). AtACBP2₂₁₅₋₃₅₄ consists of the ANK domain lacking the ACB domain. Interactions were measured by titrating 20-30 μ M AtLYSOPL2 wild-type or mutant proteins in the chamber with 300-400 μ M AtACBP2 in the syringe. The values originate from Table 3.

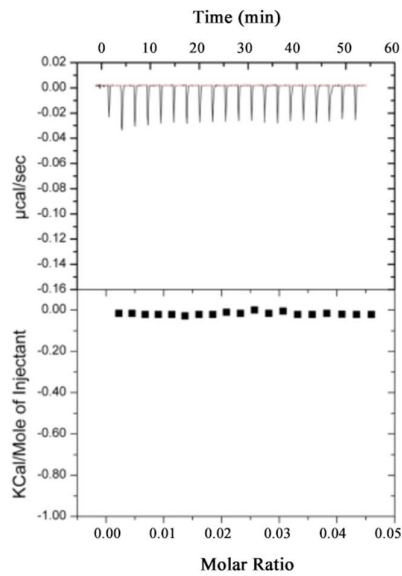


Figure S-5. ITC analysis of AtLYSOPL2 wild-type protein binding to lysoPC. ITC analysis of wild-type AtLYSOPL2 interactions with lysoPC. Interaction was measured by titrating 20-30 μM AtLYSOPL2 wild-type protein in the chamber with 600-800 μM lysoPC in the syringe. The values originate from Table 4.

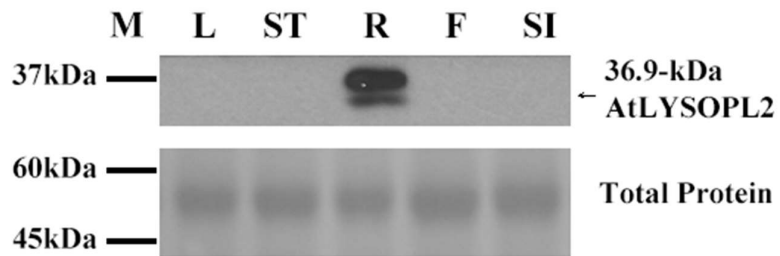


Figure S-6. Western blot analysis of AtLYSOPL2 expression in various tissues of *Arabidopsis*. Total proteins were extracted from leaves (L), stalks (ST), roots (R), flowers (F) and siliques (SI) of 5-week-old *Arabidopsis* and cross-reacted with anti-peptide antibodies against AtLYSOPL2. Bottom, gel stained with Coomassie Blue showing equal loading of protein amount in each lane. M, protein marker.

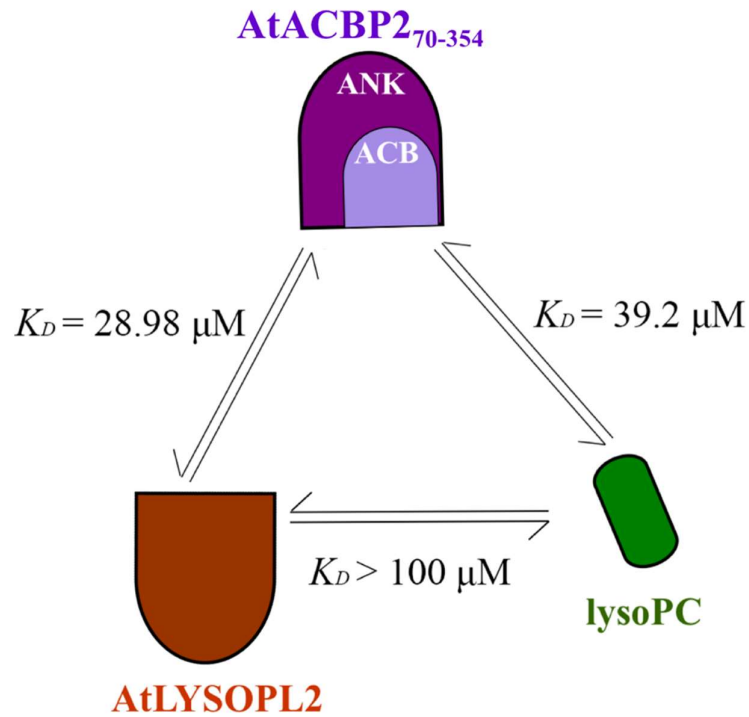


Figure S-7. Pictorial representation of the interactions between AtACBP2₇₀₋₃₅₄, AtLYSOPL2 and lysoPC. AtACBP2₇₀₋₃₅₄ binds to AtLYSOPL2 and lysoPC. LysoPC, green; ANK domain, purple; ACB domain, light purple; AtLYSOPL2, brown. The K_D values of AtACBP2₇₀₋₃₅₄ with AtLYSOPL2 and lysoPC were 28.98 μM and 39.2 μM , respectively. These values are displayed in Table 1, Table 2, Fig. 1 and Fig. 2. In comparison, the average K_D values for AtLYSOPL2 mutant proteins and lysoPC interaction were larger than 100 μM . These values are displayed in Table 4 and Fig. 6.

Table S-1. Primers used in this study.

Description	Name (Orientation)	Sequences (5' to 3')
Primer pair to amplify the coding region of <i>AtLYSOPL2</i>	ML2040 (forward)	AAACCC TGCAG CATGCCGTCGGAAGC (<i>Pst</i> I)
	ML2041 (reverse)	AGTCCAT GGT CAAGCGGTTTTAGATCC (<i>Nco</i> I)
Overlapping primer pair to introduce S1147A mutation	ML2298 (forward)	CCCAT <u>CGCT</u> TCACCAA
	ML2299 (reverse)	TTGGTGAAG <u>CGAT</u> GGG
Overlapping primer pair to introduce D268A mutation	ML2030 (forward)	CTCCAGCA <u>ATC</u> GCTGTC
	ML2031 (reverse)	GACAGCGG <u>ATG</u> CTGGAG
Overlapping primer pair to introduce H298A mutation	ML2032 (forward)	CAGCGA <u>GGC</u> ATACATCC
	ML2033 (reverse)	GGATGTAT <u>GCCT</u> CGCTG
Primer pair to amplify the coding region of <i>AtACBP2</i>	ML2037 (forward)	AAACCGG TGGAGCGG ATTCGCTTGTG (<i>Age</i> I)
	ML2039 (reverse)	AGTAAG CTTTT AGTCTGCCTGCTTTG (<i>Hind</i> III)
Primer pair to amplify the coding region of <i>AtACBP2</i> ₇₀₋₂₁₄	ML3039 (forward)	AAACCGG ATCCGCGG ATTCGCTTGTG (<i>Bam</i> HI)
	ML3040 (reverse)	AGTAAG CTTTT AGGTTCCCTTTGAGTT (<i>Hind</i> III)
Primer pair to amplify the coding region of <i>AtACBP2</i> ₂₁₅₋₃₅₄	ML3078 (forward)	ATATGA ATTCGG ACCAGTTTTTAGCTC (<i>Eco</i> RI)
	ML2039 (reverse)	AGTAAG CTTTT AGTCTGCCTGCTTTG (<i>Hind</i> III)
Primers used to screen cloned plasmids	T7 (forward)	TAATACGACTCACTATAGGG

Restriction endonuclease sties (bracketed after each sequence) are bolded. Codons for the substituted amino acids are underlined with the altered nucleotides shown in italics.